

This paper was recommended for publication in revised form by Regional Editor Sandip Kale

A NUMERICAL APPROACH FOR MODELLING THERMAL PROFILES AND EFFECTS OF PROCESS PARAMETERS ON IT IN SUBMERGED ARC WELDING OF AISI 1518 GRADE STEEL

***Abhijit Sarkar**

Research Scholar, Mechanical Engineering
Department, NIT Agartala, Tripura India

Aparesch Datta

Assistant Prof, Mechanical Engineering
Department, NIT Agartala, Tripura, India

Prasenjit Dey

Research Scholar, Mechanical
Engineering Department, NIT
Agartala, Tripura, India

R.N.Rai

Asso.prof, Production
Engineering Department, NIT
Agartala, Tripura, India

S. C Saha

Professor, Mechanical
Engineering Department, NIT
Agartala, Tripura, India

Keywords: Submerged Arc Welding (SAW), Finite Volume Method (FVM), Gaussian Heat Distribution, Transient temperature distribution, AISI 1518 grade steel.

** Corresponding author: A. Sarkar; Phone:;09615833634, E-mail address: Sarkarabhijit2014@gmail.com*

ABSTRACT

A comprehensive methodology for the analysis of thermal analysis due to welding has been studied in this present investigation. A finite volume methodology (FVM) among term of the basic heat transfer equation was enforced to simulate the temperature profiles in submerged arc welding (SAW) of AISI 1518 grade steel. The supply of the arc is assumed to be a moving conicoidal heat supply with a Gaussian distribution. The obtained results from the simulation methodology are compared with experimental results and determined a good agreement with experimental results, with associate degree overall proportion of error calculable to be between 5.23%. The influence of welding current and speed of temperature analysis has been evaluated and located that each one those parameters are playing a necessary role in moving the temperature distribution of the assembly, i.e.when current inflated, the temperature conjointly inflated with constant speed yet like higher speed temperature is decreased for constant current . Finally, the influence of heat input on peak temperature variations in various welding parameters has been evaluated and

shown that the higher heat input in higher temperature is obtained.

1. INTRODUCTION

Submerged arc fastening (SAW) is one in all the foremost common producing operations for the connection of structural parts for a several of the applications, as well as bridges, building structures, cars, trains, farm instrumentation, and nuclear reactors, to call some [1]. Studies of temperature distributions in weldments are very important for weld internal control. So, it's one in all the foremost necessary factors and sophisticated development to grasp the simulation of the heat distribution from the arc supply to the assembly. The first attempt was described in temperature distribution in weldment more than forty years ago, to model a moving point heat source for welding process. Firstly, the analytical model was developed for steady state, two dimensional heat flow problem with Fourier equation in welding and derived by Rosenthal in 1940s [2, 3]. He was assumed a point heat source model and temperature independent material thermal properties, which increase the error of the heat source model. Therefore, to

overcome these limitations several researchers has used distributed heat source models like two dimensional disc model [4], Gaussian heat distribution [5], split heat source [6], constant heat input [7], arc heat flux [8, 9], double ellipsoidal [10-13] etc. Eager and Tsai [5] improved the Rosenthal's analytical resolution of temperature distribution with introducing a moving heat supply model. Their model was a major step for the advance of temperature prediction within the close to heat supply regions. Jeong and Cho [14] have conjointly introduced an analytical resolution to conniving the transient temperature field supported the 2D Gaussian heat source, but with different distributed parameters and they have successfully transformed the solution of the temperature field in the plate of a finite thickness to the fillet welded joint.

But in practice, Welding faced many problems involve complicated geometry, thermal history with complex boundary conditions and cannot be solved analytically. Therefore, it is necessary to develop practical or numerical models for predicting the temperature distribution, for which temperature distribution can be calculated within acceptable tolerance, because a sophisticated numerical program and methods can yield accurate and reliable results [15]. Many researchers have been used in different numerical models like finite element method (FEM) [16-20] and finite difference method (FDM) [21-26] and finite difference method (FVM). More recently, in branches of thermal and mechanical strategies FVM has become a popular tool for weld modelling. In 2011, Abbas Sh Alwan [27] has been used a Finite Volume Method (FVM) for the 3D heat transfer model to determine the cooling curve in weld metal zones and temperature distribution of submerged Arc welding (SAW) process and shown that the cooling rate is influenced by welding parameters. Patankar [28] has been solved a differential governing equations of heat transfer to analysed the temperature field in the fusion zone, which is numerically solved by a finite volume method (FVM). M Kubiak [29] issues a finite volume technique numerical modelling to calculate the temperature distribution of the welded plate of Laser-arc hybrid butt-welded plates.. Zhang et al. [30] to develop a numerical heat transfer model by Finite Volume Method (FVM) to analyze the temperature profiles and the metal droplet's modelled on tungsten arc (GTA) welding process with a volumetric heat source . G Taylor et al. [31] introduce a modelled for determining the heat distribution of welding phenomena by FVM and they were shown that the temperature distribution influenced on size of fusion zone. However, developed numerical models of heat flow distribution of weldments can provide an increased understanding of the welding process, and also can provide a tool to improve processes, process control and productivity. On the other hand, the nature of thermal profile is influenced by variation on different welding parameters (such as current, voltage, welding speed etc.) [32-34]. So, it is also essential to study the influenced of process parameters on the thermal history in weldment for different welding condition. Chen et al . [35] Investigated to study the effect of weld parameters on the

thermal history in steel plates and found that welding current and voltage are effects on the temperature profiles of Weldments as well as welding speed also effects on the temperature profiles. Gery et al [36] studied on the results of fastening parameters and heat supply distribution on temperature variations in butt fastening and located that the welding speed, energy input and heat source distributions is effects on the shape and boundaries of FZ and HAZ. They also influence peak temperatures in FZ, which consequently affect the transient temperature distributions in the welded plate.

In the present investigation, a numerical model is established to analyze the temperature profiles with a moving heat source of submerged arc welding of 12 mm thick AISI 1518 grade steel by using finite volume transient heat transfer analysis. The results show that the theoretically computed data compared with experimental data is validated and gives a good agreement with experimental results of a range of welding conditions. Also, it has been described that the input parameters such as welding current and speed play an essential role in affecting the temperature distribution.

2. EXPERIMENT PROCEDURE

The specimen used for measurement of transient temperature was a rectangular piece of size 200×100×12 mm. A fused type silicon product with grain size 0.2 to 1.6 mm with basicity index 1.6 flux (AUTOMELT A55) is used for welding which having a chemical composition of, SiO₂+TiO₂=30%, CaO+ MgO =10%, Al₂O₃ + MnO= 45%, CaF₂= 15. Bead-on-plate welds were deposited using mild steel electrode coated with copper wire diameters of 3.15mm. Table 1 shows the chemical composition of the base material and electrode wire. Total fifteen (15) welds were deposited following the welding parameters given in Table 2. To measure the temperature in the welding process, the K type chromul-Aumul thermocouple was used. A sketch diagram for the submerged arc welding set up is presented in Fig. 1.

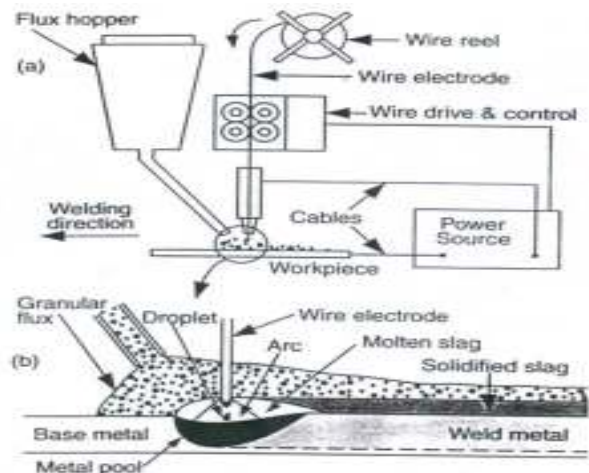


FIGURE 1: SCHEMATIC OF SAW PROCESS AND ENLARGED FIGURE OF THE ARC.

The positions of the thermocouples based on the chosen coordinate system are tabulated in Table 3. The thermocouples 1-4 were attached to a depth of 0.6 cm, through the blind holes which were drilled from the top of the plate and thermocouple 5 attached to a depth of 0.6 cm from the bottom of the plate and its schematic diagram shown in figs. 2 & 3. The temperature dependent material properties of the base metal are shown in Table 4. The density of the materials was taken of 7,850 kg/m³.

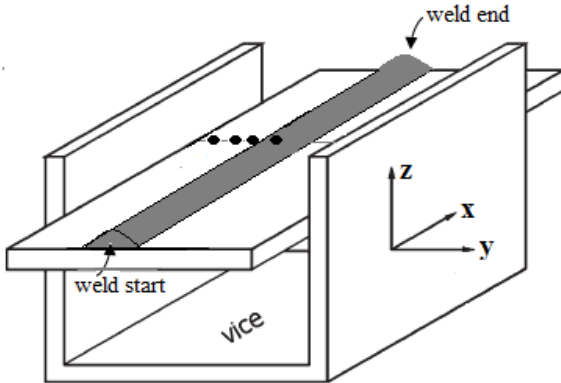


FIGURE 2: SKETCH OF WELDING PROCESS AND COORDINATE SYSTEM

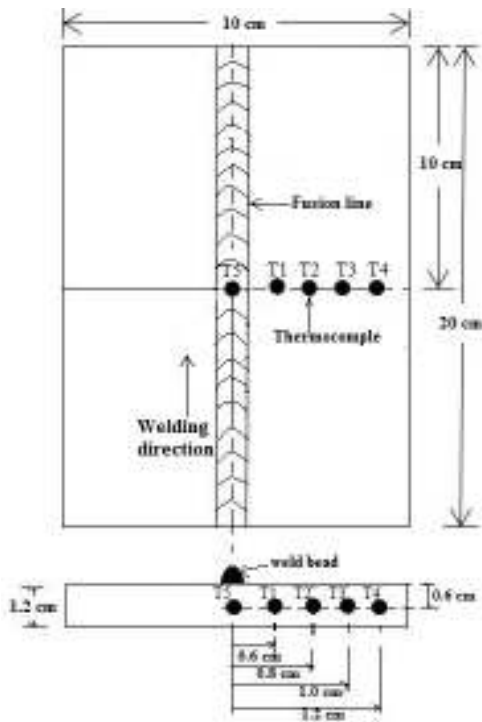


FIGURE 3 SCHEMATIC DIAGRAM OF WELDED PLATE USED IN THE EXPERIMENT

TABLE 1 CHEMICAL COMPOSITION (WT%) OF THE BASE PLATE AND ELECTRODE WIRE OF AISI 1518 GRADE STEEL

| AISI 1518 grade steel | C | Mn | Si | P | C _{eq} |
|-----------------------|-------|-----|-------|-------|-----------------|
| | 0.151 | 1.4 | 0.189 | 0.019 | 0.013 |
| Filer consumable | 0.040 | 0.4 | 0.050 | - | - |

TABLE 2: OPERATING WELDING PARAMETERS

| Ex. No | Current (A) | Voltage (V) | Welding speed (cm/Sec) |
|--------|-------------|-------------|------------------------|
| 1 | 350 | 30 | 0.67 |
| 2 | 400 | 30 | 0.67 |
| 3 | 450 | 30 | 0.67 |
| 4 | 350 | 30 | 0.75 |
| 5 | 400 | 30 | 0.75 |
| 6 | 450 | 30 | 0.75 |
| 7 | 350 | 30 | 0.80 |
| 8 | 400 | 30 | 0.80 |
| 9 | 450 | 30 | 0.80 |
| 10 | 350 | 30 | 0.95 |
| 11 | 400 | 30 | 0.95 |
| 12 | 450 | 30 | 0.95 |
| 13 | 350 | 30 | 1.00 |
| 14 | 400 | 30 | 1.00 |
| 15 | 450 | 30 | 1.00 |

TABLE 3: THERMOCOUPLE MEAN POSITION

| Thermocouple (k-type) (chromul-Aumul) | Mean position (mm) | | |
|---------------------------------------|--------------------|----|---|
| | X | Y | Z |
| T1 | 100 | 6 | 6 |
| T2 | 100 | 8 | 6 |
| T3 | 100 | 10 | 6 |
| T4 | 100 | 12 | 6 |
| T5 | 100 | 0 | 6 |

A data acquisition device was developed for the purpose of this research. A PC-based data acquisition system (NI PCIE-6351, X Series Multifunction DAQ) with a maximum frequency of 100 MHz was used to sample the signal from the thermocouples. The data acquisition system of LABVIEW was used to acquire the temperature every second, during welding from these 3 locations as well as the room temperature.

TABLE 4 TEMPERATURE DEPENDENCE OF THERMAL PROPERTIES [40]

| Temperature (°C) | Thermal conductivity (W/mK) | Specific heat (J/KgK) | Thermal expansion coefficient (10 ⁻⁶ /°C) | Enthalpy (MJ/m ³) |
|------------------|-----------------------------|-----------------------|--|-------------------------------|
| 0 | 51.9 | 450 | 10 | 0 |
| 100 | 51.1 | 499.2 | 11 | 300 |
| 200 | - | - | - | 720 |
| 300 | 46.1 | 565.5 | 12 | 1100 |
| 400 | - | - | - | 1500 |
| 450 | 41.05 | 630.5 | 13 | - |
| 500 | - | - | - | 1980 |
| 550 | 37.6 | 705.5 | 14 | - |
| 600 | 35.6 | 773.3 | 14 | 2500 |
| 700 | - | - | - | 3000 |
| 720 | 30.64 | 1080.5 | 14 | - |
| 800 | 26 | 931 | 14 | 3700 |
| 900 | - | - | - | 4500 |
| 1000 | - | - | - | 5000 |
| 1100 | - | - | - | - |
| 1450 | 29.45 | 437.93 | 15 | - |
| 1510 | 29.7 | 400 | 15 | - |
| 1580 | 29.7 | 735.5 | 15 | - |
| >2500 | - | - | - | 9000 |

3. HEAT SOURCE MODEL

3.1 Thermal modeling

In this work a transient heat governing equation is solved in the welded plate with heat generation for a homogeneous, isotropic solid in the rectangular coordinate system (x, y, z) and it can be expressed as

$$\frac{\partial}{\partial x} (K \frac{\partial T}{\partial x}) + \frac{\partial}{\partial y} (K \frac{\partial T}{\partial y}) + \frac{\partial}{\partial z} (K \frac{\partial T}{\partial z}) + q = \rho c_p \frac{\partial T}{\partial t} \quad (1)$$

Where, K is the thermal conductivity (W/m0c). Cp is the specific heat capacity (J/kg 0C), ρ is the density of the plate material (kg/m3) and q is the internal heat generation rate (W/m3), T is the unknown temperature of weld plate (0c) and is the spatial gradient operator. Considering the moving coordinate system (ξ= x - vs t), the governing equation can be rewritten as.

$$\frac{\partial}{\partial \xi} (k \frac{\partial T}{\partial \xi}) + \frac{\partial}{\partial y} (k \frac{\partial T}{\partial y}) + \frac{\partial}{\partial z} (k \frac{\partial T}{\partial z}) + q = -\rho c_p v_s (\frac{\partial T}{\partial \xi}) \quad (2)$$

$$\alpha (\frac{\partial^2 T}{\partial \xi^2} + \frac{\partial^2 T}{\partial y^2} + \frac{\partial^2 T}{\partial z^2}) + \frac{q}{\rho c_p} = -v_s (\frac{\partial T}{\partial \xi}) \quad (3)$$

Where α, thermal diffusivity of the work-piece, is equal to k/(ρcp); vs is the welding speed and t is the time.

3.2. Simulation of the Heat Source

The basic input parameter required for thermal analysis of the weld is the magnitude of the coming from the welding arc torch. Since the welding arc torch transmits heat over a surface and surface heat source (heat flux) is closer to the real condition than point heat source. Instead of uniform heat distributed, many researchers have used disc type heat source model according to Gauss distribution. For Gaussian distributed heat source, heat at certain distance (r) from centre of heat source has value according to equation 4.

$$q(r) = q_0 \exp^{-3(\frac{r}{\bar{r}})^2} \quad (4)$$

Where, q (r) is the surface heat flux at radius r, q0 is the maximum flux at the centre of the heat source. r is the concentration coefficient and the radial distance from the centre of the heat source, \bar{r} is the characteristic radial dimensional distribution parameter that defines the region in which 95 per cent of the heat flux is deposited [37]. The disc type heat distribution with conical shape represented as

$$q(r) = \frac{3Q}{\pi r^2} \exp[-3(\frac{r}{\bar{r}})^2] \quad (5)$$

Where and Q is the power of the welding heat source, V is the arc voltage, I is the welding current, η is the arc efficiency. Here, the arc efficiency is assumed to be 0.95 for submerged arc welding process [38]. When disc type heat distribution coordinate system moves with the heat source then equation (5) is replace by equation (6) [39] and it is expressed by

$$q(r, \xi) = \frac{3Q}{\pi r^2} \exp[-3(\frac{r}{\bar{r}})^2] \exp[-3(\frac{\xi}{\bar{r}})^2] \quad (6)$$

Where, is the moving coordinate system of weldments. The above equation for heat source with considering the moving coordinate system (ξ= x - vs t), equation (6) can be written as:

$$q(\xi, y, t) = \frac{3Q}{\pi r^2} \exp[-3(\frac{y}{\bar{r}})^2] \exp[-3(\frac{x - v_s t}{\bar{r}})^2] \quad (7)$$

3.3. Boundary and initial conditions

Initial and boundary conditions complete the governing equations. The finite volume modelling of the thermal behaviour during SAW performed in the present investigation is governed by the equation (1) and is subjected to the following

boundary conditions.

1. Conductive boundary condition is used for all top surface nodes, which lie on weld bead and it is defined as

$$k \frac{\partial T}{\partial n} \Big|_{Top} = q(\xi, y, t) - h(T - T_0) \quad (8)$$

2. Conductive boundary condition is used for all surface nodes, which lie on edge surface and corner except the bottom surface of the plate and it is defined as

$$-k \frac{\partial T}{\partial n} \Big|_{others} = h(T - T_0) \quad (9)$$

3. The bottom surface of the plate is taken with the ambient temperature

4. in initial condition is needed at time $t = 0$ and the initial condition can be defined as

$$T(x, y, z, 0) = T_0 \quad (10)$$

Where, T_0 is the initial temperature or pre-heat or inter-pass temperature. However, in the present work T_0 is the ambient temperature.

3.4. Assumptions

All the analyses are performed incorporating temperature dependent thermal properties of the base metal. The following assumptions are made in the formulation of the model:

1. The initial or ambient temperature of the weldments is 30°C.
2. Thermal properties of the material like density, specific heat and conductivity are temperature-dependent.
3. The convection heat transfer coefficient is taken 25 W/m²K.
4. The physical phenomena such as Maragoni effects, convective melt flow, buoyancy force and viscous force are neglected.

4. MATHEMATICAL MODEL OF TEMPERATURE DISTRIBUTION

4.1 Finite Volume Technique

The finite Volume approach is a popular choice of formulation for the advection and diffusion of the heat and material. The FV approach usually considered a subset of the Finite Difference method scientists studying flow phenomenon such as aerodynamics and hydrodynamics may choose this approach. Compressible and incompressible fluid flow regimes are examples of problems that might be modeled in a FV approach. The equation below is an example of a steady-state finite volume approximation for incompressible convection/diffusion in one dimension, where u is the variable of interest, v is velocity, and ρ are constant, x and k is space and its written as equation (11).

This equation (11) is in reality a specialized version of the Crack-Nicolson scheme, applied specially to incompressible, steady-state convection and diffusion. In this study, a mathematical model has been developed by a finite volume method (FVM) with Matlab code to simulate the temperature

profiles of weldments of submerged arc welding. Three main configurations of moving heat source over the weld surface are used: point heat source, surface heat source and volumetric heat source .In the present investigation, surface heat source based on Gaussian conicoidal heat distribution model is chosen. During welding, the welding source moves parallel to x direction with welding speed of V_s and ζ represents a moving abscissa, which is parallel to x axis in weldments as shown in figure 4. A reference section is taken at a distance of 100 mm from starting point of welding, which is related with ζ .

$$\left(\frac{\lambda}{\Delta x_{k+1}} + \frac{\lambda}{\Delta x_{k-1}} + \frac{\rho v_{k+1}}{2} - \frac{\rho v_{k-1}}{2} \right) u_k = \left(\frac{\lambda}{\Delta x_{k+1}} - \frac{\rho v_{k+1}}{2} \right) u_{k+1} + \left(\frac{\lambda}{\Delta x_{k+1}} - \frac{\rho v_{k-1}}{2} \right) u_{k-1} \quad (11)$$

4.2. Mathematical equations for different type of node

Knowledge of relative position of the reference section from the heat source (ζ) at any instant of time t is important. This is arrived by subtracting the position of heat source at that instant of time (v_s) from the distance of reference section from the starting point of the plate. The value of ζ may be positive or negative depending on the position of the heat source being before (start of welding) or after the reference section with respect to time. However it should be mentioned that heat content of the reference section changes with changing value of ζ and it is maximum at $\zeta=0$ (which means the source is above the reference section).Discretization of reference section of weldment is shown in figure 5. By considering the type of boundary condition here the unsteady state heat transfer formulation is carried out for all type of node, whether they belongs interior, surface edge or corner. Convection boundaries are considered on the surface facing the ambient as well as for those nodes which lies on the edge or corner. Heat flow among the interior node by conduction. We have surface node, interior node, corner and edge node.

The input data for this calculation included the ambient temperature, the initial temperature of the specimen, the size of the specimen and of the elements of the mesh, the initial position of the arc, the thermal properties of the specimen and environment, and the parameters which characterized the arc. A careful check for the mesh and grid independence of our numerical solutions has been made to ensure the accuracy and validity of the numerical schemes. For this purpose, in mesh systems, $t=0.05$ s and $y=z= 2$ mm, is tested. Spatial increment y , and z of 1mm, and a time step $t=0.025$ s are thus adopted in the calculation.

For all surface nodes (e.g. for node 1) has been written in equation (12). For $\Delta y=\Delta z=L$, the equation (12) become as equation (13).

For all surface nodes (e.g. for node 1)

$$h\Delta y(T_a - T_1(i)) + k\left(\frac{\Delta z}{2}\right)\left(\frac{T_2(i) - T_1(i)}{\Delta y}\right) + k\left(\frac{\Delta z}{2}\right)\left(\frac{T_2(i) - T_1(i)}{\Delta y}\right) + k\Delta y\left(\frac{T_{27}(i) - T_1(i)}{\Delta z}\right) + q\Delta y = \rho c_p \Delta y \left(\frac{\Delta z}{2}\right)\left(\frac{T_1(i+1) - T_1(i)}{t}\right) \quad (12)$$

For $\Delta y = \Delta z = L$, the equation become

$$T_1(i+1) = [1 - (2\Gamma hL/k) - 4\Gamma]T_1(i) + 2\Gamma[T_2(i) + T_{27}(i) + (hLT_a/k)] + 2L\Gamma q \quad (13)$$

where, $\Gamma = (\alpha * t) / L^2$ and $\alpha = k / \rho c_p$

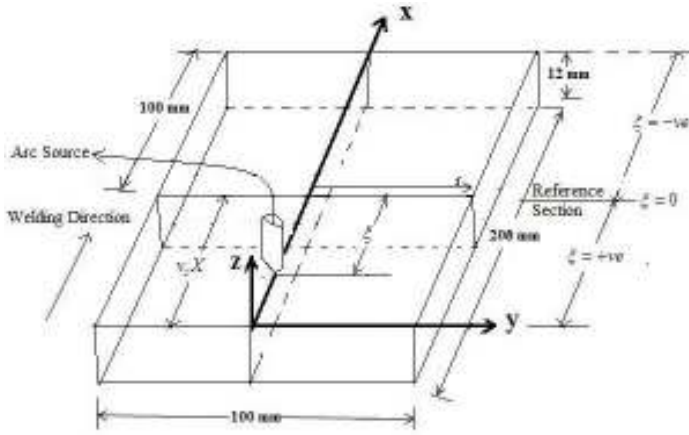


FIGURE 4 DIMENSIONS OF WELD (ALL DIMENSIONS IN MM) PLATE

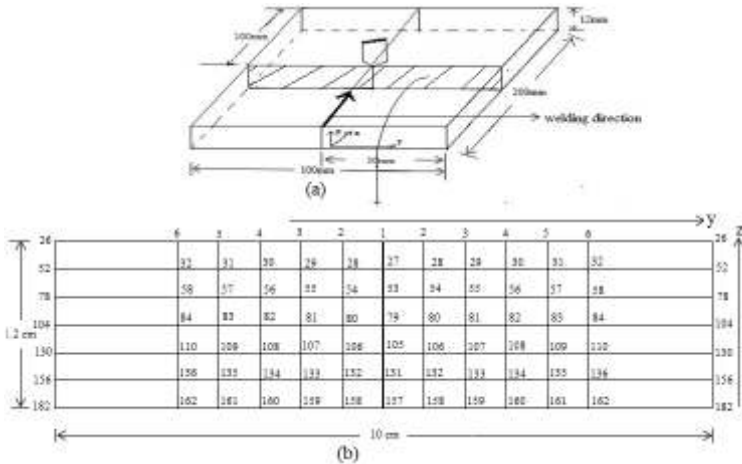


FIGURE 5 (A) PLATE WITH REFERENCE SECTION AND (B) DISCRETIZATION OF REFERENCE SECTION

Similarly for all interior, all corner and all edge nodes equation has been written as equation (14) – (19).

$$k\Delta y\left(\frac{T_1(i) - T_{27}(i)}{\Delta z}\right) + k\Delta z\left(\frac{T_{28}(i) - T_{27}(i)}{\Delta y}\right) + k\Delta z\left(\frac{T_{28}(i) - T_{27}(i)}{\Delta y}\right) + k\Delta y\left(\frac{T_{53}(i) - T_{27}(i)}{\Delta z}\right) = \rho c_p \Delta y \Delta z \left(\frac{T_{27}(i+1) - T_{27}(i)}{t}\right) \quad (14)$$

$$T_{27}(i+1) = [1 - 4\Gamma]T_{27}(i) + \Gamma[T_1(i) + 2T_{28}(i) + T_{53}(i)] \quad (15)$$

For all corner nodes (e.g. for node 26):

$$h\Delta y(T_a - T_{26}(i)) + k\left(\frac{\Delta z}{2}\right)\left(\frac{T_{25}(i) - T_{26}(i)}{\Delta y}\right) + h\left(\frac{\Delta z}{2}\right)(T_a - T_{26}(i)) + k\left(\frac{\Delta y}{2}\right)\left(\frac{T_{52}(i) - T_{26}(i)}{\Delta z}\right) = \rho c_p \left(\frac{\Delta y}{2}\right)\left(\frac{\Delta z}{2}\right)\left(\frac{T_{26}(i+1) - T_{26}(i)}{t}\right) \quad (16)$$

So,

$$T_{26}(i+1) = [1 - 4\Gamma - (4\Gamma hL/k)]T_{26}(i) + \Gamma[2T_{52}(i) + 2T_{25}(i) + (4hLT_a/k)] \quad (2)$$

For all edge nodes (e.g. for node 52):

$$h\Delta z(T_a - T_{52}(i)) + k\Delta z\left(\frac{T_{51}(i) - T_{52}(i)}{\Delta y}\right) + k\left(\frac{\Delta y}{2}\right)\left(\frac{T_{26}(i) - T_{52}(i)}{\Delta z}\right) + k\left(\frac{\Delta y}{2}\right)\left(\frac{T_{78}(i) - T_{52}(i)}{\Delta z}\right) = \rho c_p \Delta y \left(\frac{\Delta z}{2}\right)\left(\frac{T_{52}(i+1) - T_{52}(i)}{t}\right) \quad (3)$$

So,

$$T_{52}(i+1) = [1 - 4\Gamma - (2\Gamma hL/k)]T_{52}(i) + \Gamma[T_{26}(i) + T_{78}(i) + 2T_{51}(i) + (2hLT_a/k)] \quad (4)$$

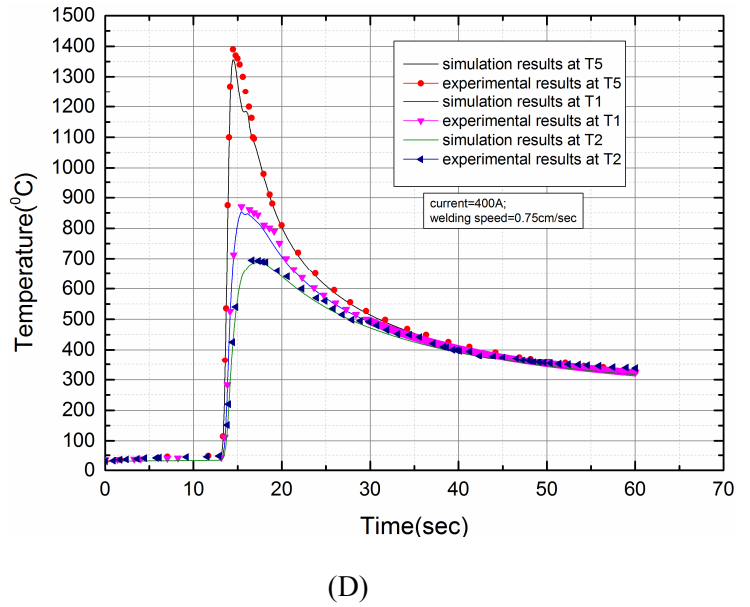
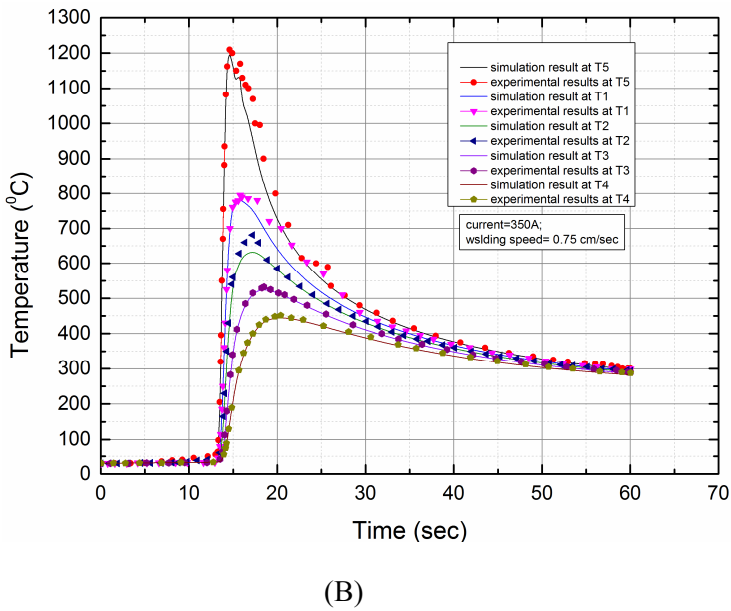
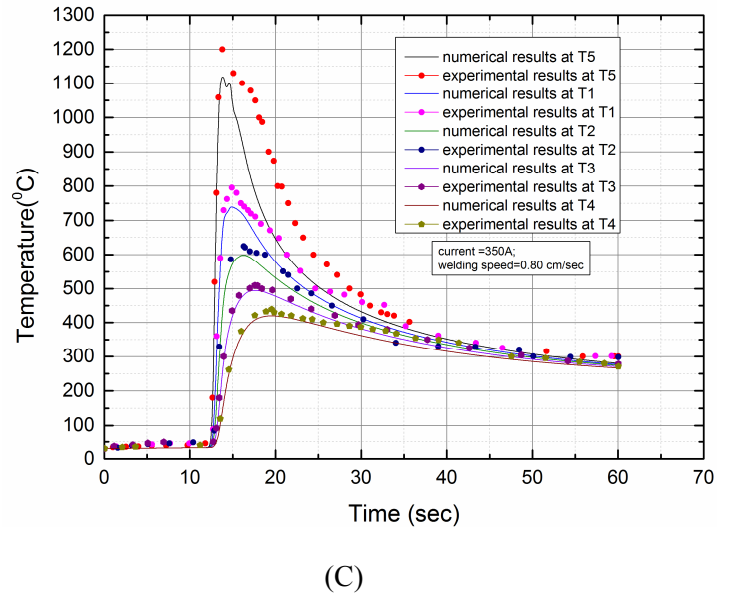
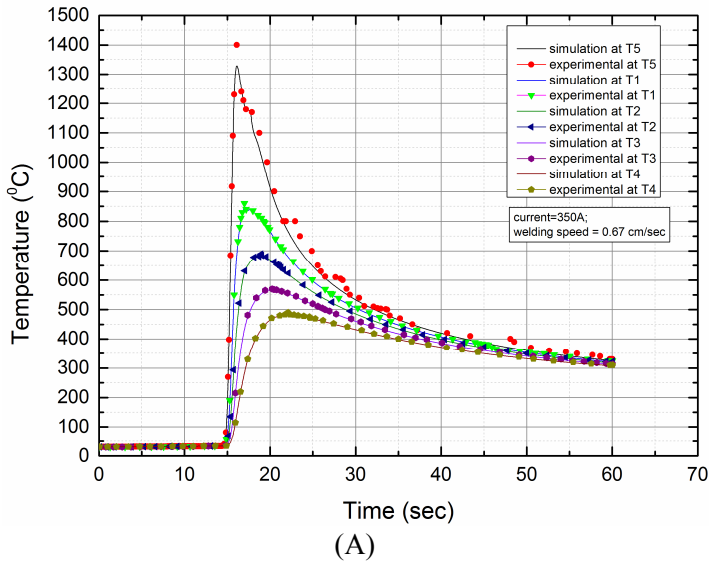
In order to ensure stability of the calculations, the mesh size and time step has to be limited. Considering equations (12)-(19), the dominant stability criteria for all nodes is expressed as

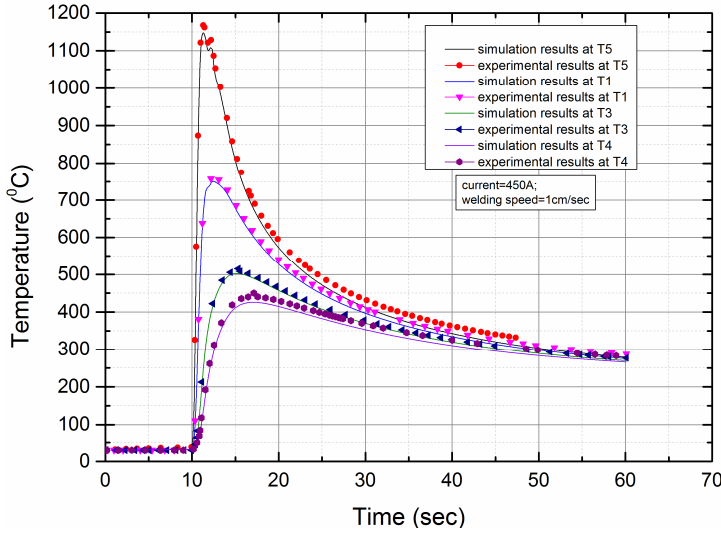
$$\Delta t \leq \frac{l^2 \rho c_p}{k} \quad (20)$$

5. RESULTS AND DISCUSSION

Figure 6 (A-E) shows the thermal profiles or temperature distribution across the transverse direction from the weld center line to the edge of the weldments. In figures 6 (A-E), comparison of simulated and measured thermal cycles at 0, 6, 8, 10 and 12 mm from weld line has shown. When the heat source reaches the weld line nodes, it rises nodes temperature to its peak value to sudden increase in temperature and cools down gradually once it moves. It should be observed that this numerical model's value lie within the theoretical ranges. From these figures it can be appealed that this simulation results has shown a good agreement with experimental results in different welding conditions. Apart from showing the general trend, the transient temperature values also match the experimental data. For the thermocouples, especially at T1, T2, T3, T4 and T5 the model predict a lower temperature than the experimental peak temperature and it may be caused by the radiation of arc source which was not modeled. The peak temperature variations for

different thermocouples with various welding parameters are provided in the table 5.





(E)

FIGURE 6 (A), (B), (C), (D) AND (E); TEMPERATURE DISTRIBUTION PROFILES AT THERMOCOUPLE T1, T2, T3, T4 AND T5 FOR DIFFERENT VALUES OF HEAT INPUT

5.1. Effect of welding current on thermal profiles

For the purpose of finding out the effects of welding process parameters on temperature distribution of weldment, with different parameters have been performed. Keeping the constant welding speed and varying the current 350A to 450A, the corresponding temperature distribution profiles are plotted for location of different thermocouples in figure 7, 8 and 9 at different locations respectively.. From these figures, it can be seen that when current increased, the temperature also increased with constant welding speed. Also shown that when the current has been changed from 350 to 450A at constant speed, with an overall percentage of change of temperature estimated to be within 19-23%.

The temperature is inversely proportional to the welding speed [27]. Therefore, when the welding speed is slower the temperature is larger, for a constant current. In case of effects of welding speed condition, the temperature distributions in the weldment at T5, T1, T2, T3 and T4 for constant current (350A or 400A or 450A) for variant welding speeds, 0.67-1 cm/s is shown in figure 10,11 & 12. From figure 8, it can be concluded that with higher speed, temperature is decreases in the weldment as the heat source applies for a shorter period of time when it moves faster.

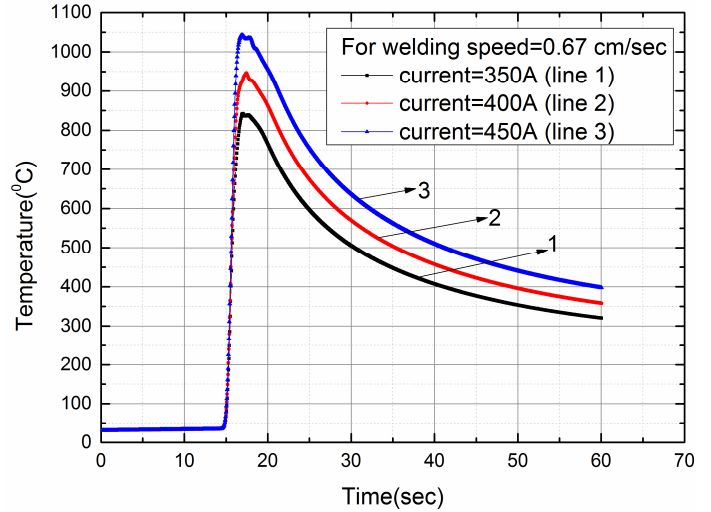


FIGURE 7 TEMPERATURE DISTRIBUTION PROFILE VARY CURRENT WITH CONSTANT WELDING SPEED 0.67 CM/SEC AT T1

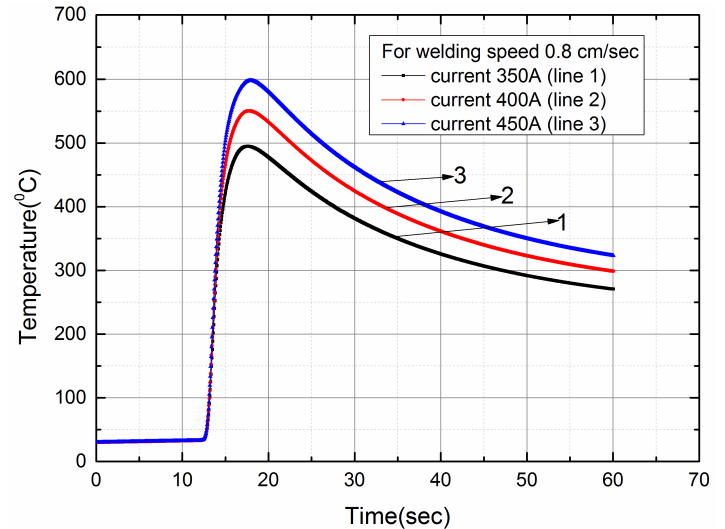


FIGURE 8 TEMPERATURE DISTRIBUTION PROFILE VARY CURRENT WITH CONSTANT WELDING SPEED 0.80 CM/SEC AT T3

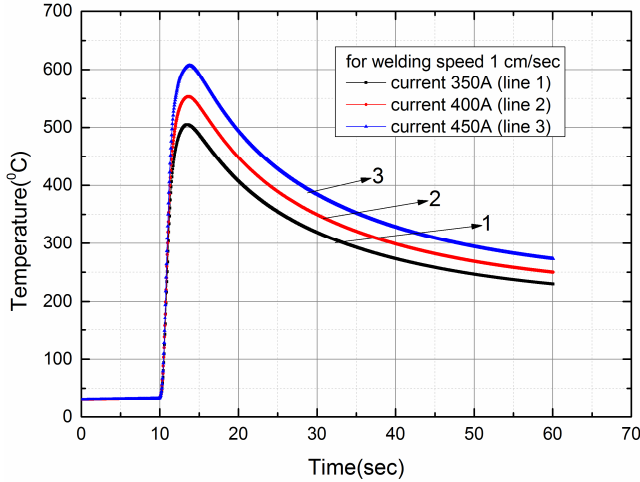


FIGURE 9 TEMPERATURE DISTRIBUTION PROFILE VARY CURRENT WITH CONSTANT WELDING SPEED 1CM/SEC AT T3.

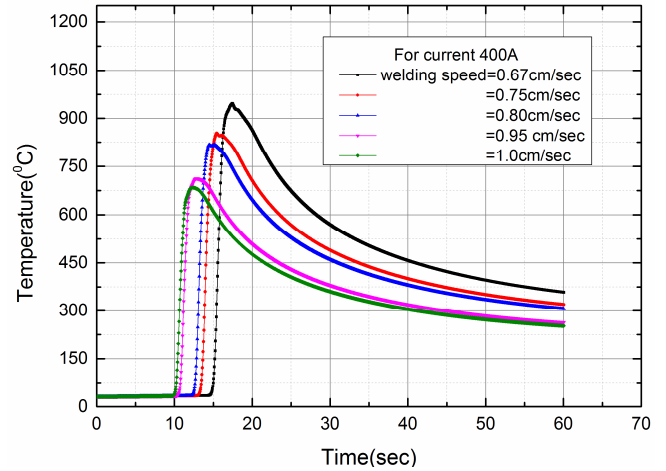


FIGURE 11 EFFECT OF WELDING SPEED ON TEMPERATURE DISTRIBUTION AT T1 (ALL DIMENSIONS IN CM) FOR DIFFERENT VALUES OF WELDING SPEED WITH CONSTANT WELDING CURRENT 400A.

5.2. Effect of welding speed on thermal profiles

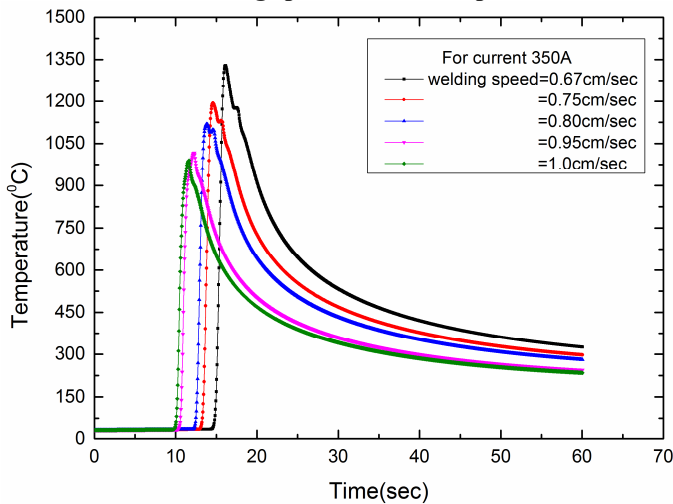


FIG. 10: EFFECT OF WELDING SPEED ON TEMPERATURE DISTRIBUTION AT T5 (ALL DIMENSIONS IN CM) FOR DIFFERENT VALUES OF WELDING SPEED WITH CONSTANT WELDING CURRENT 350A.

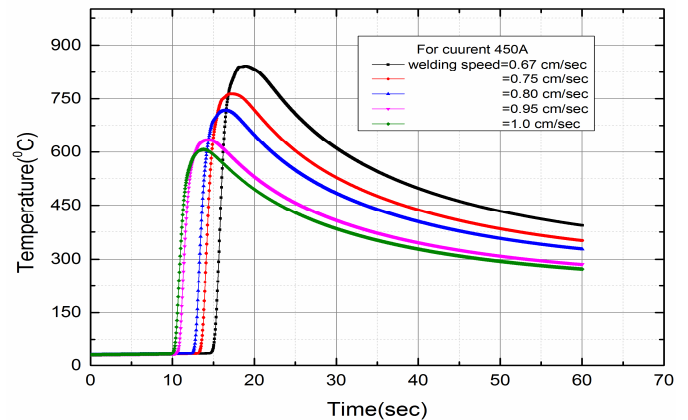


FIGURE 12: EFFECT OF WELDING SPEED ON TEMPERATURE DISTRIBUTION AT T2 (ALL DIMENSIONS IN CM) FOR DIFFERENT VALUES OF WELDING SPEED WITH CONSTANT WELDING CURRENT 450A.

5.3. Effects of heat input on peak temperature

The heat input has obvious effects thermal profiles of weldments and the change in temperature is approximately directly proportional to the heat input. For the purpose of finding out the effects of heat input on peak temperature, with different welding parameters have been performed. For corresponding the peak temperature distributions with varying the heat input to 1 to 1.92 KJ/mm at thermocouples T1,T2,T3,T4 & T5 are plotted in figure 13. From figure 13, it can be seen that the higher heat input results in higher temperature.

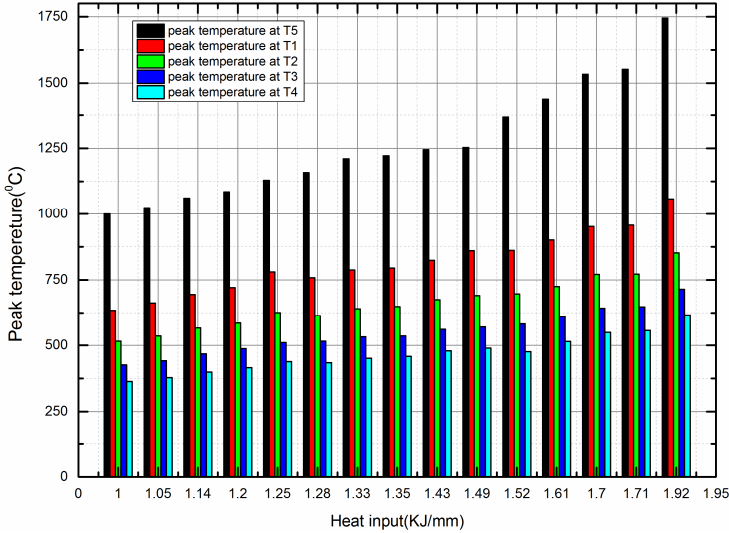


FIGURE 13 PEAK TEMPERATURE VARIATION FOR VARIOUS THERMOCOUPLES AT DIFFERENT WELDING PARAMETERS

6. CONCLUSION

In this study, a systematic procedure was followed to perform the thermal analysis for submerged arc welding of AISI 1518 grade steel. A moving heat source model based on Gaussian heat source model was implemented in matlab code and validated with experimental results. Heat source fitting analysis results of the FVM model was validated by using numerical procedure and its accuracy was demonstrated from the peak temperature measurement on plate welds. Based on the result and discussion the following conclusions may be drawn:

1. The mathematical model for thermal profile is predicted reliably in points out of the weldment.
2. The predicted temperature distribution is validated against the experimental results obtained by thermal model, and they are found to be in a good agreement.
3. The maximum percentage error between experimental and numerical data is found at 5.23%.
4. The distances between the center of welding line and the location where the peak temperature occurs increases slightly as the current is increased, but decrease with the increase of the welding speed.
5. Peak temperature variation for various thermocouples at different welding parameters are influenced by heat input
6. From parametric result, it can be concluded that the temperature profiles is increasing for welding speed decrease as well as the current increases.
7. This method can be used in future developments to select the process and the welding parameters that meet the thermal necessities of the plan.
8. The model is tested may be extended for other materials as well as other joint geometries.

NOMENCLATURE

| | |
|-----------------|--|
| ρ | Density, kg/m ³ |
| c_p | Heat capacity, J/kgK |
| k_x, k_y, k_z | Thermal conductivity, W/mK |
| x, y, z | Space coordinate, m |
| Q | Heat generated, W |
| r | Radial distance from the centre, m |
| \bar{r} | Characteristic radial dimensional distribution parameter |
| h | Heat transfer coefficient, W/m ² K |
| η | thermal efficiency, % |
| Z | ZenerHollomon parameter s ⁻¹ |
| ξ | Moving coordinate axis, m |
| v_s | Welding Speed, m/s |
| q | Heat flux, W/m ² |
| T | Temperature, K |

ACKNOWLEDGMENTS

The author offers his sincere thanks to Prof. S.C. Saha of Mechanical Engineering Department and Instructors of Workshop, NIT, Agartala for their valuable help in finishing this work.

REFERENCES

- [1] P. T. Houldcroft, Submerged-arc welding: Woodhead Publishing, 1989.
- [2] D. Rosenthal, "Mathematical theory of heat distribution during welding and cutting," Welding journal, vol. 20, pp. 220s-234s, 1941.
- [3] D. Rosenthal, "The theory of moving sources of heat and its application to metal treatments," 1946.
- [4] V. Pavelic, R. Tanbakuchi, O. Uyehara, and P. Myers, "Experimental and computed temperature histories in gas tungsten-arc welding of thin plates," WELD J, vol. 48, p. 295, 1969.
- [5] T. Eagar and N. Tsai, "Temperature fields produced by traveling distributed heat sources," Welding Journal, vol. 62, pp. 346-355, 1983.
- [6] M. A. Wahab, M. Painter, and M. Davies, "The prediction of the temperature distribution and weld pool geometry in the gas metal arc welding process," Journal of Materials Processing Technology, vol. 77, pp. 233-239, 1998.
- [7] S. Murugan, P. Kumar, and B. Raj, "Temperature distribution during multipass welding of plates," International journal of pressure vessels and piping, vol. 75, pp. 891-905, 1998.
- [8] R. Choo, J. Szekely, and R. Westhoff, "On the calculation of the free surface temperature of gas-tungsten-arc weld pools from first principles: Part I. Modeling the welding arc," Metallurgical Transactions B, vol. 23, pp. 357-369, 1992.
- [9] H. Fan, H.-L. Tsai, and S. Na, "Heat transfer and fluid flow in a partially or fully penetrated weld pool in gas tungsten arc welding," International Journal of Heat and Mass Transfer, vol. 44, pp. 417-428, 2001.

- [10] P. Duranton, J. Devaux, V. Robin, P. Gilles, and J. Bergeau, "3D modelling of multipass welding of a 316L stainless steel pipe," *Journal of Materials Processing Technology*, vol. 153, pp. 457-463, 2004.
- [11] J. Goldak, A. Chakravarti, and M. Bibby, "A new finite element model for welding heat sources," *Metallurgical transactions B*, vol. 15, pp. 299-305, 1984.
- [12] N. Nguyen, A. Ohta, K. Matsuoka, N. Suzuki, and Y. Maeda, "Analytical solutions for transient temperature of semi-infinite body subjected to 3-D moving heat sources," *WELDING JOURNAL-NEW YORK-*, vol. 78, pp. 265-s, 1999.
- [13] S. Wen, P. Hilton, and D. Farrugia, "Finite element modelling of a submerged arc welding process," *Journal of Materials Processing Technology*, vol. 119, pp. 203-209, 2001.
- [14] S. Jeong and H. Cho, "An analytical solution to predict the transient temperature distribution in fillet arc welds," *Welding Journal-Including Welding Research Supplement*, vol. 76, p. 223s, 1997.
- [15] C. K. Takemori, D. T. Muller, and M. A. d. Oliveira, "Numerical simulation of transient heat transfer during welding process," 2010.
- [16] A. Anca, A. Cardona, J. Risso, and V. D. Fachinotti, "Finite element modeling of welding processes," *Applied Mathematical Modelling*, vol. 35, pp. 688-707, 2011.
- [17] S. Bag, A. Trivedi, and A. De, "Development of a finite element based heat transfer model for conduction mode laser spot welding process using an adaptive volumetric heat source," *International Journal of Thermal Sciences*, vol. 48, pp. 1923-1931, 2009.
- [18] S. Kumar and S. Bhaduri, "Three-dimensional finite element modeling of gas metal-arc welding," *Metallurgical and Materials Transactions B*, vol. 25, pp. 435-441, 1994.
- [19] E. Nart and Y. Celik, "A practical approach for simulating submerged arc welding process using FE method," *Journal Of Constructional Steel Research*, vol. 84, pp. 62-71, 2013.
- [20] N. S. Shanmugam, G. Buvanashakaran, K. Sankaranarayanan, and S. R. Kumar, "A transient finite element simulation of the temperature and bead profiles of T-joint laser welds," *Materials & Design*, vol. 31, pp. 4528-4542, 2010.
- [21] S. M. Adedayo and S. Irehovbude, "Numerical simulation of transient temperature in flash butt-welded axisymmetric circular sections," *Journal of Naval Architecture and Marine Engineering*, vol. 10, pp. 33-40, 2013.
- [22] M. H. Al-Sa'ady, M. A. Abdulsattar, and L. S. Al-Khafagy, "Finite difference simulation of low carbon steel manual arc welding," *Thermal Science*, vol. 15, pp. 207-214, 2011.
- [23] K. Boo and H. Cho, "Transient temperature distribution in arc welding of finite thickness plates," *Proceedings of the Institution of Mechanical Engineers, Part B: Journal of Engineering Manufacture*, vol. 204, pp. 175-183, 1990.
- [24] P. Ghadimi, H. Ghassemi, M. Ghassabzadeh, and Z. Kiaei, "Three-dimensional simulation of underwater welding and investigation of effective parameters," *Welding journal*, vol. 92, 2013.
- [25] A. Grill, "The thermal history of a composite cylinder girth welded by TIG," *International Journal for Numerical Methods in Engineering*, vol. 18, pp. 1031-1044, 1982.
- [26] W. Grzesik and M. Bartoszuk, "Prediction of temperature distribution in the cutting zone using finite difference approach," *International Journal of Machining and Machinability of Materials*, vol. 6, pp. 43-53, 2009.
- [27] D. A. S. Alwan, "Reliability of numerical analysis of cooling curves in the fusion zone of submerged arc welding (saw) process," *The Iraqi Journal for Mechanical And Material Engineering*, vol. 11, pp. 672-682, 2011.
- [28] S. Patankar, *Numerical heat transfer and fluid flow*: CRC Press, 1980.
- [29] M. Kubiak, "Numerical modelling of liquid material flow in the fusion zone of hybrid welded joint."
- [30] W. Zhang, G. Roy, J. Elmer, and T. DebRoy, "Modeling of heat transfer and fluid flow during gas tungsten arc spot welding of low carbon steel," *Journal of Applied Physics*, vol. 93, pp. 3022-3033, 2003.
- [31] G. A. Taylor, M. Hughes, N. Strusevich, and K. Pericleous, "Finite volume methods applied to the computational modelling of welding phenomena," *Applied Mathematical Modelling*, vol. 26, pp. 311-322, 2002.
- [32] D. B. Darmadi, A. K. Tieu, and J. Norrish, "A validated thermal model of bead-on-plate welding," *Heat and Mass Transfer*, vol. 48, pp. 1219-1230, 2012.
- [33] A. Ghosh, S. Chattopadhyaya, and N. Singh, "Prediction of weld bead parameters, transient temperature distribution & HAZ width of submerged arc welded structural steel plates," in *Defect and Diffusion Forum*, 2012, pp. 405-409.
- [34] R. Komanduri and Z. Hou, "Thermal analysis of the arc welding process: Part I. General solutions," *Metallurgical and Materials Transactions B*, vol. 31, pp. 1353-1370, 2000.
- [35] B. Chen, M. Adak, and C. G. Soares, "Numerical investigations to study the effect of weld parameters on the temperature-time history in steel plates," *Acoustic Analyses Using Matlab® and Ansys®*, p. 285, 2014.
- [36] D. Gery, H. Long, and P. Maropoulos, "Effects of welding speed, energy input and heat source distribution on temperature variations in butt joint welding," *Journal of Materials Processing Technology*, vol. 167, pp. 393-401, 2005.
- [37] A. Okada, "Application of melting efficiency and its problems," *Journal of Japan Welding Society*, vol. 46, pp. 53-61, 1977.
- [38] K. Easterling, *Introduction to the physical metallurgy of welding*: Elsevier, 2013.
- [39] G. Krutz and L. Segerlind, "Finite Element Analysis of Welded Structures," *SAE Technical Paper* 1976.
- [40] Pathak AK, Datta GL. Three-dimensional finite element analysis to predict the different zones of

microstructures in submerged arc welding. Proc Inst Mech
Engrs J Eng Manufact B 2004;218:269–80.